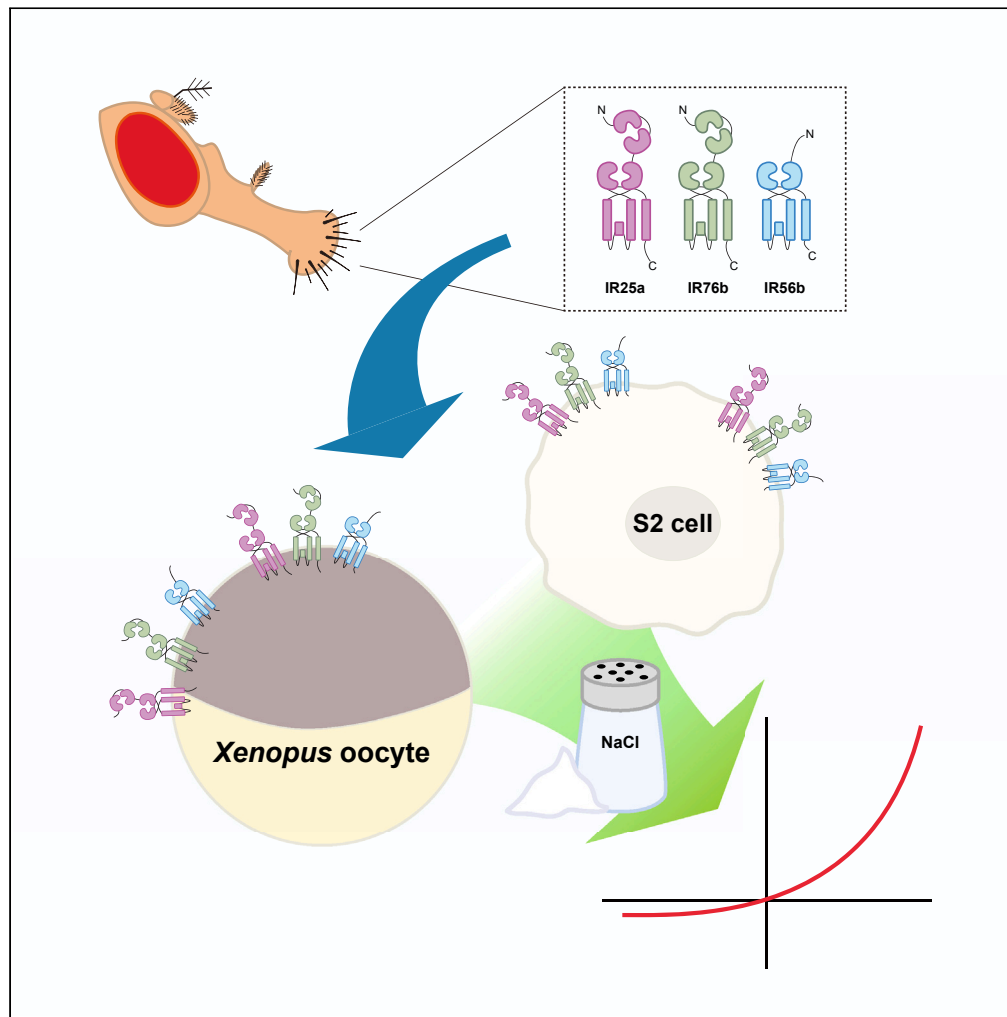


Article

# Molecular and cellular basis of sodium sensing in *Drosophila* labellum



Wayessa Rahel Asefa, Jin-Nyeong Woo, Seon Yeong Kim, ..., Byung-Chang Suh, KyeongJin Kang, Jae Young Kwon

bcsuh@dgist.ac.kr (B.-C.S.)  
kangkj@kbri.re.kr (K.K.)  
jykwon@skku.edu (J.Y.K.)

**Highlights**

Sugar neurons in L sensilla cf. responses to NaCl, but not those in S-c sensilla

*Ir56b* mutant shows impaired physiological responses to NaCl in the *Drosophila* labellum

*Ir56b* is involved in attraction behavior induced by low concentrations of NaCl

*Ir76b*, *Ir25a*, and *Ir56b* can form a complex that responds to NaCl in heterologous systems



## Article

Molecular and cellular basis  
of sodium sensing in *Drosophila* labellum

Wayessa Rahel Asefa,<sup>1,8</sup> Jin-Nyeong Woo,<sup>2,8</sup> Seon Yeong Kim,<sup>2,3,8</sup> Hyungjun Choi,<sup>1,8</sup> Hayeon Sung,<sup>1,4</sup> Min Sung Choi,<sup>1</sup> Minkook Choi,<sup>5</sup> Sung-Eun Yoon,<sup>6</sup> Young-Joon Kim,<sup>6,7</sup> Byung-Chang Suh,<sup>2,\*</sup> KyeongJin Kang,<sup>3,\*</sup> and Jae Young Kwon<sup>1,9,\*</sup>

## SUMMARY

**Appropriate ingestion of salt is essential for physiological processes such as ionic homeostasis and neuronal activity. Generally, low concentrations of salt elicit attraction, while high concentrations elicit aversive responses. Here, we observed that sugar neurons in the L sensilla of the *Drosophila* labellum cf. responses to NaCl, while sugar neurons in the S-c sensilla do not respond to NaCl, suggesting that gustatory receptor neurons involved in NaCl sensing may employ diverse molecular mechanisms. Through an RNAi screen of the entire *Ir* and *ppk* gene families and molecular genetic approaches, we identified IR76b, IR25a, and IR56b as necessary components for NaCl sensing in the *Drosophila* labellum. Co-expression of these three IRs in heterologous systems such as S2 cells or *Xenopus* oocytes resulted in a current in response to sodium stimulation, suggesting formation of a sodium-sensing complex. Our results should provide insights for research on the diverse combinations constituting salt receptor complexes.**

## INTRODUCTION

Salt ingestion is essential for multiple physiological processes, such as neuronal excitation, transmembrane transport of organic compounds in diverse tissues, and osmotic homeostasis. Excessive salt intake often disrupts these intricate functions, posing significant challenges to the overall well-being of the organism. As an example, elevated Na<sup>+</sup> ion concentration has been implicated in the onset of various health concerns, including hypertension, gastrointestinal cancer, osteoporosis, and autoimmune disorders.<sup>1–4</sup> Therefore, the regulation of appropriate salt consumption is essential. Many animals are known to prefer salt up to 100 mM NaCl, but to gradually dislike it at higher concentrations.<sup>5–8</sup> In mice, low concentrations of sodium salt (<100 mM) are mainly sensed by amiloride-sensitive epithelial sodium channels (ENaC) expressed on the apical surface of taste receptor cells.<sup>5</sup> In contrast, high salt taste acts as an aversive cue through the bitter and sour taste pathways in mice.<sup>7</sup>

The *Drosophila* labellum has been a valuable research model due to its ability to detect a wide range of tastes including salt. The labellum is composed of 31 taste sensilla categorized into three classes based on their length: long (L-type), short (S-type), and intermediate (I-type). L- and S-type sensilla possess four gustatory receptor neurons (GRNs), while I-type sensilla have two GRNs.<sup>9–11</sup> Sugars, bitter compounds, or water (osmolarity) each elicit responses in subsets of GRNs, whereas in the case of NaCl, all GRN types exhibit dose-dependent excitation or inhibition by salt.<sup>8,12</sup>

In the fly labellum, two cell types exhibit low salt tuning properties. Sugar neurons respond to higher concentrations of sodium but display a relatively low threshold for sodium activation, making them responsible for appetitive behavior induced by low sodium concentrations.<sup>8,13</sup> Additionally, it is known that *Ionotropic receptor 94e* (*Ir94e*)-*GAL4*-expressing GRNs are also activated by low sodium concentrations.<sup>8</sup>

Two other cell types, bitter GRNs and *pickpocket23* (*ppk23*)-expressing glutamatergic GRNs, act as high salt GRNs, responding to high salt concentrations and promoting avoidance behavior.<sup>8,14</sup> At the molecular level, IR76b is known to be expressed in many GRNs, forming a core complex with IR25a. The core complex together with IR56b induces an attractive response to low concentration salt,<sup>13</sup> while the core complex with IR7c induces an aversive response to high concentrations of salt.<sup>14</sup>

In this study, we delve into the comprehensive characterization of NaCl-responsive gustatory sensilla in the *Drosophila* labellum. Through selective inactivation and rescue experiments using specific *GAL4* drivers, we discovered that in the L sensilla, sugar-sensing neurons account for the majority of NaCl responses. However, in the S-c sensilla, among the neurons expressing *Ir76b-GAL4*, neurons other than the

<sup>1</sup>Department of Biological Sciences, Sungkyunkwan University, Suwon 16419, Republic of Korea

<sup>2</sup>Department of Brain Sciences, Daegu Gyeongbuk Institute of Science and Technology (DGIST), Daegu 42988, Republic of Korea

<sup>3</sup>Neurovascular Unit Research Group, Korea Brain Research Institute, Daegu 41062, Republic of Korea

<sup>4</sup>Department of Molecular, Cellular and Developmental Biology, College of Literature, Science, and the Arts, The University of Michigan, Ann Arbor, USA

<sup>5</sup>Department of Oral Biology, Yonsei University College of Dentistry, Seoul 03722, Republic of Korea

<sup>6</sup>Korea Drosophila Resource Center, Gwangju 61005, Republic of Korea

<sup>7</sup>School of Life Sciences, Gwangju Institute of Science and Technology (GIST), Gwangju 61005, Republic of Korea

<sup>8</sup>These authors contributed equally

<sup>9</sup>Lead contact

\*Correspondence: bcsuh@dgist.ac.kr (B.-C.S.), kangkj@kbri.re.kr (K.K.), jykwon@skku.edu (J.Y.K.)

<https://doi.org/10.1016/j.isci.2024.110248>



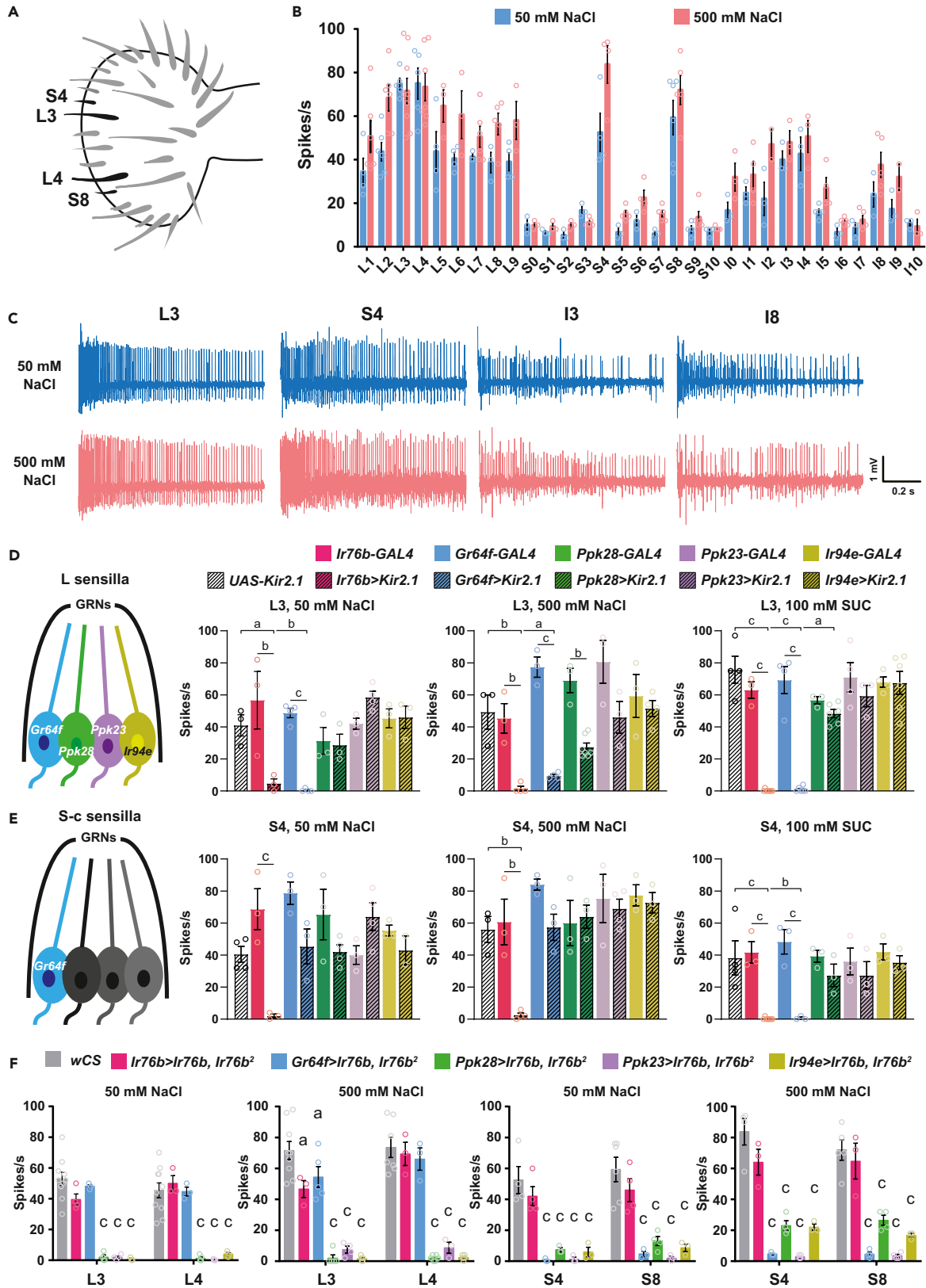


**Figure 1. Salt response of gustatory receptor neurons in the *Drosophila* labellum**

(A) Schematic representation of taste sensilla on the fly labellum.

(B) Control wCS labellar taste sensilla responses to 50 mM and 500 mM NaCl.  $n = 3-9$ . All spikes, regardless of amplitude, were counted for quantification. The L- and S-type sensilla showed spikes of relatively similar amplitudes, while the I-type sensilla showed spikes of diverse amplitudes, large and small.

(C) Sample traces of recordings from (B).

(D and E) Schematic representation illustrating the four gustatory receptor neurons (GRNs) constituting the L sensilla (D) and S-c sensilla (E), each labeled with respective GAL4 drivers (left). Responses to NaCl and sucrose when specific GRNs were inactivated using the indicated GAL4 drivers and UAS-Kir2.1.  $n = 3-10$ . One-way ANOVA was followed by Tukey's post-hoc test.

(F) Responses to NaCl upon GRN-specific rescue using the indicated GAL4 drivers in the *Ir76b* mutant.  $n = 3-10$ . Two-way ANOVA was followed by Dunnett's multiple comparison test. Statistical analyses compared each group with control wCS (gray bar). Bars in all figures represent the SEM, and open circles represent data points. a:  $p < 0.05$ , b:  $p < 0.01$ , c:  $p < 0.001$ .

sugar-sensing GRNs detect NaCl. These findings suggest the presence of distinct NaCl-sensing neuronal populations in the labellum, potentially indicating the existence of independent receptor complexes for NaCl detection. Previous studies implicated the *Ir* and *ppk* gene families in salt sensing in *Drosophila*, prompting us to conduct an RNAi screen targeting these gene families.<sup>8,13-18</sup> Also, we targeted the *Irs* expressed in the labellum as candidates and identified receptors essential for NaCl sensing.<sup>19</sup> Using molecular genetics and electrophysiological approaches, we verified the essential roles of *IR76b*, *IR25a*, and *IR56b* for NaCl detection in the *Drosophila* labellum. Furthermore, upon ectopically expressing these three IRs in *S2* cells and *Xenopus* oocytes, we observed the generation of currents in response to NaCl, demonstrating their capacity to form a functional NaCl receptor complex.

**RESULTS****NaCl responses in labellar taste neurons**

In the *Drosophila* labellum, about 31 bristles exist on each side of the left and right hemispheres, which are generally classified into three types based on their length (Figure 1A). *Drosophila* labellar sensilla were found to elicit responses to both low and high concentrations of NaCl (Figure 1B).<sup>8,13,14,17,18</sup> Overall, all nine L-type sensilla showed robust responses to NaCl, with L3 and L4 exhibiting particularly stronger responses to 50 mM NaCl (Figure 1B). Among the S-type sensilla, S-c sensilla (S4 and S8) showed exceptionally strong responses, while the remaining sensilla exhibited weak responses of less than 20 spikes/sec, consistent with previous studies (Figure 1B).<sup>13,17,18</sup> Since the S-c sensilla do not respond at all to bitter compounds, in contrast to the other S-type sensilla,<sup>20</sup> and respond strongly and specifically to NaCl, we focused on the S-c sensilla. The response to NaCl in I-type sensilla varied depending on the sensillum (Figure 1B). I-type sensilla have two neurons, one of which responds to sugars and low salt, and the other to bitters and high salt.<sup>21</sup> Both neurons can be activated by NaCl, resulting in a larger amplitude due to the summation of coincident spikes in response to NaCl (Figure 1C). The response to NaCl in I-type sensilla is quite complex, with considerable inter-individual variation and the production of action potentials of multiple amplitudes. Thus, we conducted subsequent experiments specifically targeting the L and S-c type sensilla which show relatively easily interpreted responses. To test the specificity of these salt responses in the L and S-c type sensilla, we tested for responses to 50 mM and 500 mM concentrations of KCl and sodium acetate. For KCl, a mild response was observed only in response to the high concentration, while sodium acetate caused physiological responses at the lower concentration, suggesting that the NaCl responses are elicited by  $\text{Na}^+$  and not by  $\text{Cl}^-$  (Figure S1).

Each L-sensilla is composed of four chemosensory neurons, which have been shown to be labeled by *Gr64f-GAL4* (sugar), *ppk28-GAL4* (water), *ppk23-GAL4* (high salt), and *Ir94e-GAL4* (low salt) through reporter expression and calcium imaging studies (Figure 1D).<sup>8</sup> We utilized these reagents to identify neurons responsible for the electrophysiological responses to NaCl. First, we performed functional ablation of each taste neuron using *Kir2.1*, an inward rectifying potassium channel, and measured NaCl responses. Notably, when *Ir76b-GAL4*-expressing neurons within the L sensilla were inactivated by UAS-Kir2.1, NaCl responses nearly vanished. Inactivated *Gr64f-GAL4*-expressing sugar-sensing neurons showed a weak residual response to 500 mM NaCl, and no response to 50 mM NaCl. Responses to 100 mM sucrose were also absent only when the function of *Ir76b*- or *Gr64f-GAL4*-expressing neurons was impaired. In addition, when the function of water sensing neurons was impaired using *ppk28-GAL4*, responses to both low and high concentrations of NaCl were slightly reduced (Figure 1D and S2).

Previous studies demonstrated that gustatory responses to low salt, high salt, calcium, acids, amino acids, fatty acids, and polyamines require the presence of *IR76b*.<sup>17,18,22-24</sup> Consistent with its widespread involvement in the taste system, *Ir76b-Gal4* appears to be expressed in every tested type of GRN.<sup>8</sup> *IR76b* was also shown to play an essential role in salt detection and *Ir76b* mutants are unable to detect salt.<sup>8,14,17,18</sup> Thus, we attempted to rescue the lack of salt response in the *Ir76b* mutant by expressing *IR76b* specifically in individual neurons using GAL4 drivers in *Ir76b* mutant flies, and found that NaCl responses were restored only when *Ir76b*- or *Gr64f-GAL4* were used (Figure 1F). Based on these results, it appears that sugar-sensing GRNs account for the majority of NaCl responses in the L sensilla, at least in our experimental paradigm.

S-c sensilla also have four neurons, one of which is labeled by *Gr64f-GAL4* and characterized as a sugar-sensing neuron, while the remaining three neurons have not been fully characterized.<sup>8</sup> Similar to our approach with L sensilla, we investigated the NaCl response in S-c sensilla neurons by selectively inactivating or rescuing specific neurons using GAL4 drivers in the *Ir76b* mutant. In contrast to L sensilla, when *Gr64f-GAL4*-expressing neurons were inactivated, the response to sucrose was completely abolished, but the response to NaCl remained intact. The response to NaCl was only absent when *Ir76b-GAL4*-expressing neurons were inactivated (Figure 1E and S2). While the *Ir76b-GAL4* driver fully rescued NaCl responses in the *Ir76b* mutant, *Gr64f-GAL4* did not (Figure 1F). These results suggest that in the S-c sensilla, neurons other than sugar-sensing neurons, specifically those expressing *Ir76b-GAL4*, cf. responses to NaCl.

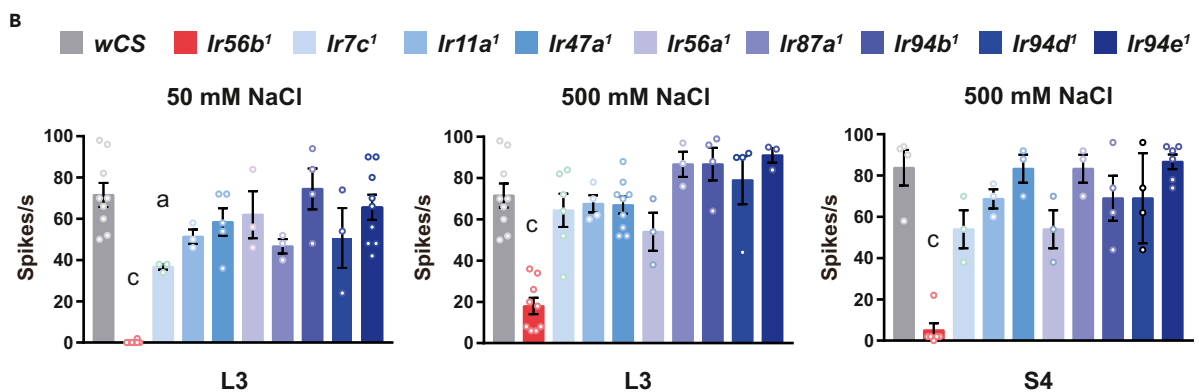
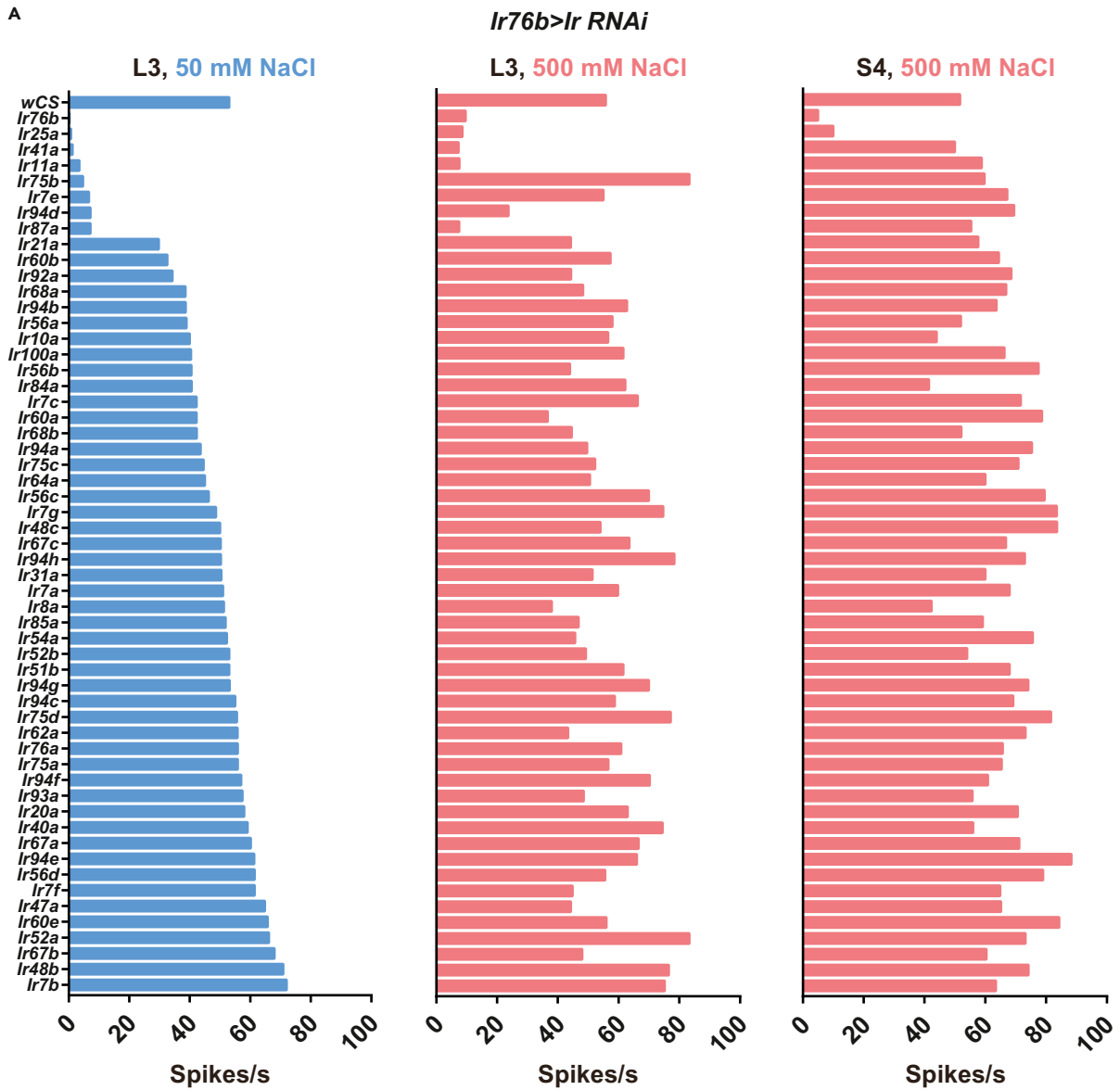


**Figure 2. Identification of *Ir56b* as a receptor necessary for NaCl detection in labellar sensilla**

(A) The average values of labellar NaCl responses in progeny from crosses between the *Ir76b*-GAL4 driver and each *Ir* RNAi line. The control, wCS, is positioned at the top, followed by an increasing amplitude of responses starting from *Ir76b* RNAi, which has the smallest response to 50 mM NaCl in the L3 sensillum.  $n = 3-15$ . (B) NaCl responses of *Ir* mutants. Error bars are the SEM and open circles are data points. Two-way ANOVA followed by Dunnett's multiple comparison test;  $n = 3-9$ . Each group compared with control wCS (gray bar). a:  $p < 0.05$ , c:  $p < 0.001$ .

**Three ionotropic receptors are necessary for NaCl responses in L and S-c sensilla**

Based on our experiments, it appeared that sugar-sensing neurons in the L sensilla detect NaCl, while in the S-c sensilla, *Ir76b*-GAL4-expressing neurons, not sugar neurons, detect NaCl. This led us to speculate that there may be independent receptor complexes for NaCl sensing in these two types of neurons. To investigate this possibility, we conducted an RNAi screen with *Irs* and *ppk* genes as candidates using two concentrations of NaCl, 50 mM and 500 mM. We expressed individual *Ir*-RNAi constructs in all NaCl-sensing neurons using *Ir76b*-GAL4, and measured the electrophysiological responses to 50 mM and 500 mM NaCl in L3 and L4 sensilla, as well as the response to 500 mM NaCl in S4 and S8 of the S-c sensilla (Figure 2A). Compared to the wCS control, *Ir76b* and *Ir25a* RNAi showed significantly reduced responses in all cases, consistent with previous studies indicating an essential role of these two receptors in salt detection (Figure 2A).<sup>8,14,17,18</sup> In L sensilla, *Ir11a*, *Ir41a*, *Ir87a*, and *Ir94d* RNAi resulted in reduced responses to both 50 mM and 500 mM NaCl, while *Ir7e* and *Ir75b* RNAi specifically reduced responses to 50 mM NaCl (Figure 2A). In S-c sensilla, apart from *Ir25a* and *Ir76b* RNAi, no other *Ir* RNAi showed a significantly reduced response to 500 mM NaCl (Figure 2A).

We also investigated *ppk* RNAi using the same approach. While we did not find any *ppk* genes which RNAi significantly reduced the response to NaCl in S-c sensilla, *ppk3* and *ppk22* RNAi resulted in reduced responses to both 50 mM and 500 mM NaCl in L sensilla. Additionally, *ppk8*, *ppk13*, *ppk14*, and *ppk25* RNAi specifically reduced the response to 50 mM NaCl (Figure S3A). However, since the *ppk* RNAi lines that decreased the response to 50 mM NaCl in L sensilla also exhibited reduced responses in UAS-RNAi control flies (Figure S3B), we did not proceed with further experiments regarding the *ppk* genes.

Next, we examined *Ir* mutants as an additional means to identify and verify the *Ir* genes necessary for NaCl detection. In addition to the candidates identified in the RNAi screen, we also included *Ir* genes known to be expressed in the labellum based on previous studies<sup>19</sup> as part of our candidate selection. Ultimately, we generated mutants for the following *Ir* genes: *Ir7c*, *Ir11a*, *Ir47a*, *Ir56a*, *Ir56b*, *Ir87a*, *Ir94b*, *Ir94d*, and *Ir94e*. Among these *Ir* gene mutants, only the *Ir56b* mutant showed reduced responses to both low and high concentrations of NaCl in all sensilla compared to the control (Figure 2B). In the *Ir*-RNAi line screen, *Ir56b* RNAi showed a response to NaCl comparable to the control, but the *Ir56b* mutant was clearly defective in salt responses. This is likely due to low efficiency of RNAi.

We further investigated whether *Ir56b* is essential for NaCl detection in the *Drosophila* labellum. Both the *Ir56b* mutant we generated and the insertion mutant obtained from the Bloomington *Drosophila* Stock Center showed reduced NaCl responses in all L- and S-type sensilla (Figure 3A). Almost no response was observed to NaCl, ranging from low (10 mM NaCl) to high concentrations (500 mM NaCl) (Figures 3B and 3C). However, the introduction of wild-type IR56b rescued the responses (Figures 3D and 3E). Similar to the *Ir76b* mutant, the *Ir56b* mutant exhibited no issues with aversive behavior toward high concentration NaCl (500 mM), but showed defective preference behavior toward low concentration NaCl (50 mM) (Figure 3F and S4). This behavioral defect in response to NaCl was also rescued by introducing wild-type IR56b (Figure 3F). The *Ir56b* mutant showed responses comparable to control wCS flies for sugar (100 mM sucrose and trehalose) and bitter (1 mM lobeline and 5 mM caffeine) stimuli, indicating that the impairment observed was specifically for NaCl (Figure S5). As previously reported, *Ir76b*-GAL4 labels almost all of the labellar taste neurons, including sugar sensing neurons (*Gr64f-lexA* expressing neurons). Although most of the *Ir56b*-GAL4 expressing neurons appear to be a subset of the sugar-sensing neurons, we cannot rule out the possibility that neurons expressing only IR56b exist (Figure S6). The role of *Ir56b* in sodium sensing was previously reported,<sup>13</sup> but we independently identified *Ir56b* as a salt sensor through construction of nine *Ir* mutants from candidates from our RNAi screen and candidates reported to be expressed in the labellum. In summary, in the fruit fly labellum, *Ir56b*, *Ir76b*, and *Ir25a* are necessary for physiological activation in response to NaCl in both L and S-c sensilla.

**Three ionotropic receptors can form a functional NaCl receptor complex**

To investigate whether the three IRs can form a receptor complex sufficient for NaCl detection, we used S2 cells and *Xenopus* oocytes. Initially, we attempted to use cDNA clones of the three *Ir* genes and HEK293T cells, because a previous study had shown that IR76b-expressing HEK293T cells showed an increased current in whole-cell recordings.<sup>17</sup> However, no current was observed even when the three IRs were all expressed in HEK293T cells. Since bitter receptor complexes were successfully expressed in S2 cells and observed to show a current,<sup>25,26</sup> we decided to use S2 cells. In addition, a recent study showed that *Ir56b* has an atypical structure with a minimal N-terminal region (NTR), unlike other IRs. It is encoded by a pseudo-pseudogene with translational readthrough of a premature termination codon (PTC).<sup>13</sup> In the same study, *Ir56b* was found to be a gene that generates a single exon transcript that includes an annotated 51 bp intron in the *Ir56b* transcript, and translational readthrough of the PTC in the *Ir56b* gene was verified.<sup>13</sup> We hypothesized that the *Ir56b* cDNA we used was non-functional and thus constructed a new cDNA with an intron that substituted the PTC with TTC, which encodes phenylalanine. To measure ionotropic receptor-dependent currents, we performed a whole-cell patch clamp in S2 cells transfected with *Ir* genes and EGFP. The cells were held at a holding potential of 0 mV and depolarized from -100 mV to 100 mV in 20 mV increments for 200 ms. S2 cells transfected with EGFP alone generated a small current density ( $4.65 \pm 2.426$  pA/pF) at 100 mV. However, S2 cells transfected with *Ir* genes elicited an almost 6 times larger current density ( $30.12 \pm 2.426$  pA/pF) than control cells at the same voltage (Figure 4A). The recorded current was considered a non-selective cation current generated by the *Ir* genes, since the current-voltage graph was a straight line that passed through the zero point (Figure 4B), and the

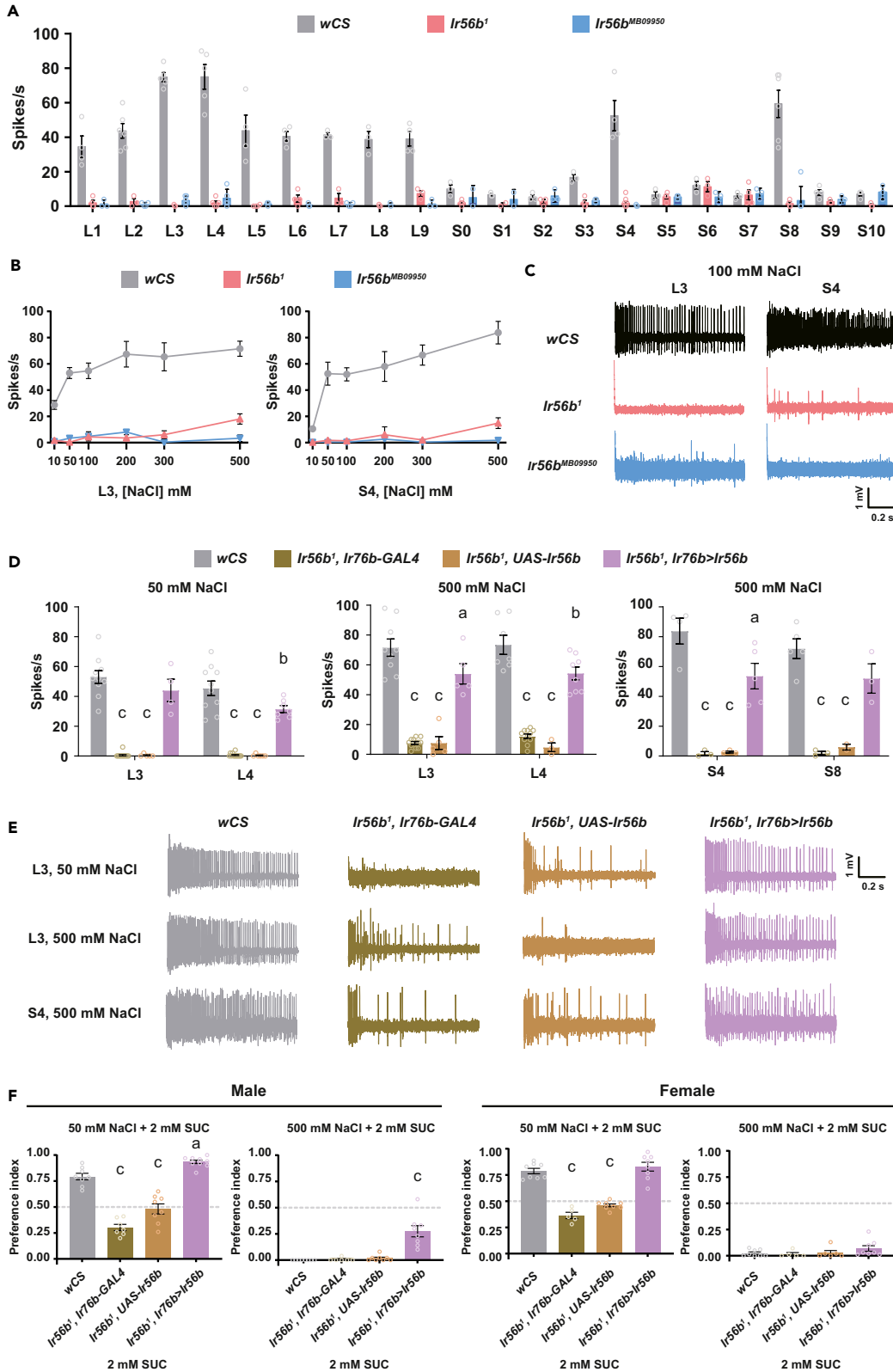




**Figure 3. *Ir56b* is necessary for NaCl sensing**

- (A) Responses to 50 mM NaCl in control *wCS*, *Ir56b*<sup>1</sup>, and *Ir56b*<sup>MB09950</sup> flies. *n* = 3–10. The values for the control are from Figure 1B.
- (B) Responses to various concentrations of NaCl in control *wCS*, *Ir56b*<sup>1</sup>, and *Ir56b*<sup>MB09950</sup> flies.
- (C) Representative traces of recordings in response to 100 mM NaCl.
- (D) NaCl responses of L and S-c sensilla for the indicated genotypes. Error bars are the SEM and open circles are data points. Two-way ANOVA followed by Dunnett's multiple comparison test; *n* = 3–12. a: *p* < 0.05, b: *p* < 0.01, c: *p* < 0.001.
- (E) Sample traces of recordings from (D).
- (F) Two-way preference behavioral responses to NaCl for the indicated genotypes. Error bars are the SEM and open circles are data points. One-way ANOVA followed by Sidak's multiple comparison test; *n* = 5–9. a: *p* < 0.05, c: *p* < 0.001. All statistical analyses compared each data point with control *wCS* (gray bar).

only freely transferable cations were the Na<sup>+</sup> and Cs<sup>+</sup> ions based on the experimental solution conditions. We also tested whether the heterologous expression of the three ionotropic receptors in *Xenopus laevis* oocytes correlates with current responses to increased NaCl concentrations. Suggesting difficulty of heterologous expression of the IRs, only two out of five trials of cRNA microinjection significantly produced currents from the oocytes expressing IR56b TTC, IR76b, and IR25a in response to 80 and 100 mM NaCl (Figure 5). However, coinjection of cRNA generated from the spliced version of *Ir56b* cDNA with those of *Ir76b* and *Ir25a* did not yield current increases in response to up to 100 mM NaCl compared to the water injection control (Figure 5). This result suggests that IR56b tunes the IR complex with its coreceptors to detect concentration changes of NaCl.

**DISCUSSION**

In this study, we conducted a screen to identify receptors essential for NaCl detection in the *Drosophila* labellum, targeting the *Ir* and *ppk* gene families. After identifying *Ir56b* as a crucial component in NaCl sensing, we demonstrated that IR56b, IR76b, and IR25a can form a functional receptor complex capable of generating currents in response to NaCl in a heterologous system.

Initially, we used electrophysiological methods to identify GRNs activated by NaCl in the *Drosophila* labellum. Taken together, our experimental results show that in the L-sensilla, sugar-sensing neurons play an important role in detecting NaCl, in particular, low concentrations of NaCl. Inactivation of sugar-sensing GRNs almost completely abolishes the response to NaCl, and *Gr64f-GAL4*-driven IR76b expression in the *Ir76b* mutant restores the physiological response to NaCl. However, since a residual response to 500 mM NaCl is observed when sugar-sensing neurons are inactivated (Figure 1D), and the *Ir56b* mutant avoids 500 mM NaCl (Figure 3F), we cannot rule out the possibility that more than one sodium-sensing neuron is present in the L sensilla, similar to previous studies.<sup>8,14,27</sup>

Salt sensing is not a simple labeled line system like sugar or bitter taste, but induces varying behavioral responses depending on concentration.<sup>8</sup> In the *Drosophila* labellum, certain neurons are inhibited by sodium, while some are activated, and certain neurons respond to both low and high salt. Therefore, future research should aim to precisely define the functions of different subsets of GRNs in salt sensing under various physiological conditions. While salt taste coding is undoubtedly complex, a point of consensus is that in the *Drosophila* labellum, sugar neurons primarily react to low sodium concentrations, and bitter GRNs act as concentrations increase. This sweet GRN-mediated preference for low concentrations and bitter GRN-mediated aversion to high concentrations is not unique to salt but is also thought to apply to fatty acids such as hexanoic acid.<sup>22</sup> In real life situations, sweetness can become aversive at very high concentrations, and bitter and sour tastes can be appetitive at low concentrations. It would be interesting to investigate whether the brain perceives other taste modalities differently depending on concentration, in a similar manner to salt, as this is a commonly observed phenomenon in the olfactory system but has been less explored in the taste system.

Until now, research on fly salt sensing has primarily focused on molecular mechanisms involving the *Ir* genes, but IR-independent salt avoidance mechanisms also clearly exist. Our behavioral experiment results, as well as those of other studies, show that high concentrations of NaCl (500 mM) are avoided by both the *Ir76b* and *Ir56b* mutants.<sup>13</sup> Furthermore, in the case of IR7c, which has been proposed to potentially form a functional high salt receptor with IR76b and IR25a, *Ir7c* mutants also exhibit high salt avoidance.<sup>14</sup> Additionally, even when bitter-sensing neurons that can detect high concentrations of NaCl independently of *Ir76b* are inactivated in the *Ir76b* mutant background, flies still avoid 500 mM NaCl.<sup>27</sup> It is possible that pharyngeal GRNs are involved in this response or that avoidance is due to changes in osmolality, or that a toxic stimulus is perceived as pain. A recent study reported that a single pair of pharyngeal neurons that express *Ir60b* control the ingestion of high salt.<sup>28</sup> Furthermore, sugar GRNs have been suggested to be inhibited by high concentrations of salt.<sup>27</sup> As such, salt taste coding might be influenced by the interaction among GRNs within a single sensillum.

Since RNAi of *Ir76b* or *Ir25a*, which were previously known to be essential for salt sensing, resulted in a lack of electrophysiological response in both L sensilla and S-c sensilla, we initially expected that a screen using the *Ir* RNAi lines would yield additional components involved in salt sensing. However, when mutants of candidate *Ir* genes obtained from the RNAi screen were constructed and tested, the mutants showed a normal NaCl response. A possible explanation is that *Ir* RNAi had resulted in an overall inhibition of neuronal function, including the response to salt, or a developmental defect. *Ir56b* RNAi showed a response to NaCl identical to the control, which may have been due to low efficiency of RNAi.

In a previous study, bitter neurons responded to NaCl in a dose-dependent manner upon ectopic expression of IR56b in bitter-sensing neurons of the labellum, whereas IR56b expression did not elicit a response to any concentration of NaCl in an *Ir25a* or *Ir76b* mutant background.<sup>13</sup> These results suggest that IR56b, IR76b, and IR25a act together to enable a response to NaCl. In this study, we suggest that these three receptors can form a functional sodium receptor complex by observing currents upon heterologous expression of these receptors in S2 cells and *Xenopus* oocytes, although not in the context of native fly GRNs. Specifically, when we introduced *Ir76b*, *Ir25a*, and *Ir56b* cDNAs into



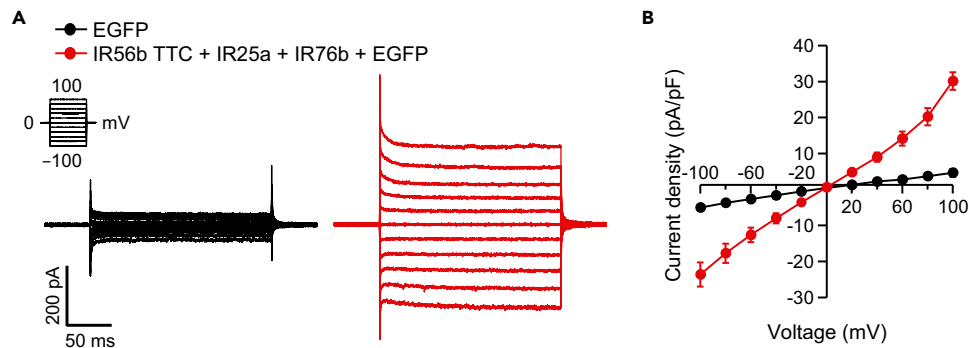


**Figure 4. IR56b TTC + IR76b + IR25a elicited Na<sup>+</sup> currents in S2 cells**

(A) Families of representative voltage-dependent current traces in S2 cells transfected with EGFP alone (black) or IR56b TTC, IR76b, IR25a, and EGFP (red). The cells were held at a holding potential of 0 mV, and depolarizing voltage steps were applied from  $-100$  mV to  $100$  mV in  $20$  mV increments for  $200$  ms. (B) Current-voltage relationship of S2 cells expressing EGFP alone (black,  $n = 3$ ) or IR56b TTC, IR76b, IR25a, and EGFP (red,  $n = 7$ ).

HEK293T cells or *Xenopus* oocytes, no current was observed in response to sodium. Currents were observed when IR76b, IR25a, and IR56b TTC were co-expressed in *Xenopus* oocytes and S2 cells, suggesting that all three components are essential. Strikingly, it should be noted that cells appear to become sick when these receptors are expressed in S2 cells. EGFP was co-transfected when transfecting S2 cells, and S2 cells expressing GFP looked sick compared to non-GFP-expressing cells. This may be due to the influence of salt present in the media. For these reasons, we were unable to test various receptor combinations under more diverse conditions. Nonetheless, we believe that our study provides a foundation for future research on receptor properties in heterologous systems.

### Limitations of the study

We systematically investigated GRNs responding to NaCl, but it is still not entirely clear which individual GRN type induces specific behavioral responses depending on salt concentration. The study of GRNs that respond to NaCl in S-c type sensilla is particularly challenging because of a lack of specific drivers. In our study, experiments using *GAL4* transgenes and electrophysiology of the *Ir76b* mutant show that *Gr64f-GAL4* negative neurons in the S-c sensilla are responsible for NaCl responses, and that the *Ir56b* mutant is necessary for the NaCl response in S-c sensilla. It would be ideal to be able to clearly show the existence of *Gr64f*-negative and *Ir56b*-positive neurons in the S-c sensilla, but this is difficult due to the limitations of reagents currently available. In a recent study, *Ir7c*, which is known to be necessary for high salt detection, was found to be expressed within the L-type subset of the *ppk23<sup>lut</sup>* population as well as in a non-glutamatergic GRN in each of the S4 and S8 sensilla.<sup>14</sup> These S4 and S8 non-glutamatergic GRNs may potentially be the salt-sensing neurons in S-c sensilla that are *Ir76b-GAL4* positive and *Gr64f-GAL4* negative, and it is possible that *Ir7c* and *Ir56b* act together in these neurons, but this requires further investigation. Using a heterologous system to study the biophysical mechanisms by which *Ir56b* and *Ir7c* subunits cf. changes in both ion selectivity and sensitivity to a salt-taste receptor is necessary, but we were unable to address this due to technical challenges.

### STAR★METHODS

Detailed methods are provided in the online version of this paper and include the following:

- KEY RESOURCES TABLE
- RESOURCE AVAILABILITY
  - Lead contact
  - Materials availability
  - Data and code availability
  - *Drosophila* stocks and transgenic flies
  - Electrophysiology
  - Behavioral assays
  - S2 cell culture and transfection
  - Whole-cell recording of S2 cells
  - Whole-cell recording of HEK293T cells
  - Patch clamp in *Xenopus* oocytes
  - Immunostaining and microscopy

### SUPPLEMENTAL INFORMATION

Supplemental information can be found online at <https://doi.org/10.1016/j.isci.2024.110248>.

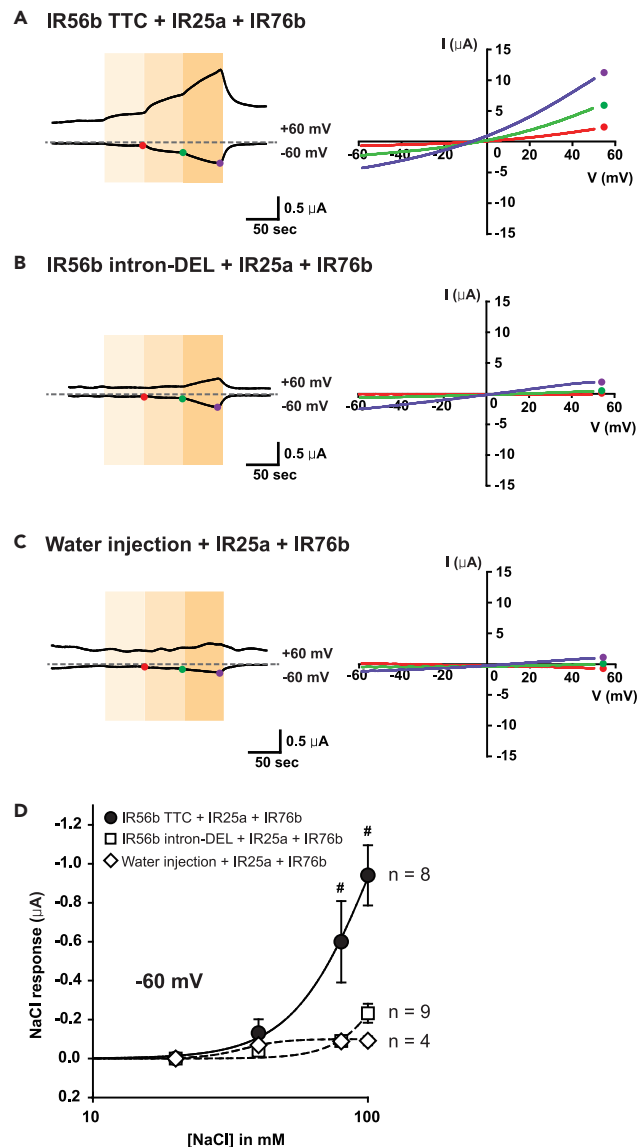


**Figure 5. IR56b TTC + IR76b + IR25a elicited  $\text{Na}^+$  currents in *Xenopus oocytes***

(A–C) Representative dose dependence (left) and current-voltage relationship (right) of NaCl responses in *Xenopus oocytes* heterologously expressing the indicated combinations of IRs. Note that the time scales and dose sequences are set identical for simple comparison of activation kinetics. IV curves were obtained at 40 (red), 80 (green), and 100 mM (purple) NaCl.

(D) The currents from the recordings in (A–C) are plotted and fitted. See the text for details. The data were fitted to the Hill equation to determine EC50s. Tukey's and Mann-Whitney U or Student's t tests were performed. # $p < 0.05$ .

## ACKNOWLEDGMENTS

We thank the Bloomington *Drosophila* Stock Center for providing flies. This work was supported by the National Research Foundation of Korea (NRF) grant NRF-2021R1A2C1011696 and 2022M3E5E8017946 (to J.Y.K.), 2020R1A4A1019436 (to J.Y.K. and B.-C.S.), 2022R1A2C100656012 and RS-2024-00351000 (to B.-C.S.), and 2021R1A2B5B01002702 (to K.J.K); and Korea Brain Research Institute 23-BR-01-02 (to K.J.K) funded by the Ministry of Science and ICT.

## AUTHOR CONTRIBUTIONS

W.R.A., J.-N.W., S.Y.K., H.C., H.S., M.S.C., M.C., S.-E.Y., Y.-J.K., B.-C.S., K.J.K., and J.Y.K. conceived the study. J.Y.K. carried out the initial experimental design. R.A.W., J.-N.W., S.Y.K., H.C., H.S., and M.C. conducted all the experiments and performed data analysis. R.A.W.,

J.-N.W., S.Y.K., H.C., M.S.C., S.-E.Y., and Y.-J.K. analyzed the data. B.-C.S., K.J.K, and J.Y.K. supervised the project. R.A.W., J.-N.W., S.Y.K., H.C., M.S.C., B.-C.S., K.J.K, and J.Y.K. wrote the manuscript.

## DECLARATION OF INTERESTS

The authors declare no competing interests.

Received: November 12, 2023

Revised: March 14, 2024

Accepted: June 7, 2024

Published: June 11, 2024

## REFERENCES

- Frisoli, T.M., Schmieder, R.E., Grodzicki, T., and Messerli, F.H. (2012). Salt and hypertension: is salt dietary reduction worth the effort? *Am. J. Med.* 125, 433–439. <https://doi.org/10.1016/j.amjmed.2011.10.023>.
- Tsugane, S., Sasazuki, S., Kobayashi, M., and Sasaki, S. (2004). Salt and salted food intake and subsequent risk of gastric cancer among middle-aged Japanese men and women. *Br. J. Cancer* 90, 128–134. <https://doi.org/10.1038/sj.bjc.6601511>.
- He, F.J., and MacGregor, G.A. (2008). Salt intake and cardiovascular disease. *Nephrol. Dial. Transplant.* 23, 3382–3385. , discussion 3385. <https://doi.org/10.1093/ndt/gfn550>.
- Kleinewietfeld, M., Manzel, A., Titze, J., Kvakon, H., Yosef, N., Linker, R.A., Muller, D.N., and Hafler, D.A. (2013). Sodium chloride drives autoimmune disease by the induction of pathogenic TH17 cells. *Nature* 496, 518–522. <https://doi.org/10.1038/nature11868>.
- Chandrashekar, J., Kuhn, C., Oka, Y., Yarmolinsky, D.A., Hummler, E., Ryba, N.J.P., and Zuker, C.S. (2010). The cells and peripheral representation of sodium taste in mice. *Nature* 464, 297–301. <https://doi.org/10.1038/nature08783>.
- Lindemann, B. (2001). Receptors and transduction in taste. *Nature* 413, 219–225. <https://doi.org/10.1038/35093032>.
- Oka, Y., Butnaru, M., von Buchholtz, L., Ryba, N.J.P., and Zuker, C.S. (2013). High salt recruits aversive taste pathways. *Nature* 494, 472–475. <https://doi.org/10.1038/nature11905>.
- Jaeger, A.H., Stanley, M., Weiss, Z.F., Musso, P.Y., Chan, R.C., Zhang, H., Feldman-Kiss, D., and Gordon, M.D. (2018). A complex peripheral code for salt taste in *Drosophila*. *Elife* 7, e37167. <https://doi.org/10.7554/eLife.37167>.
- Freeman, E.G., and Dahanukar, A. (2015). Molecular neurobiology of *Drosophila* taste. *Curr. Opin. Neurobiol.* 34, 140–148. <https://doi.org/10.1016/j.conb.2015.06.001>.
- Scott, K. (2018). Gustatory Processing in *Drosophila melanogaster*. *Annu. Rev. Entomol.* 63, 15–30. <https://doi.org/10.1146/annurev-ento-020117-043331>.
- Stocker, R.F. (1994). The organization of the chemosensory system in *Drosophila melanogaster*: a review. *Cell Tissue Res.* 275, 3–26. <https://doi.org/10.1007/BF00305372>.
- Montell, C. (2021). *Drosophila* sensory receptors—a set of molecular Swiss Army Knives. *Genetics* 217, 1–34. <https://doi.org/10.1093/genetics/iyaa011>.
- Dweck, H.K.M., Talross, G.J.S., Luo, Y., Ebrahim, S.A.M., and Carlson, J.R. (2022). Ir56b is an atypical ionotropic receptor that underlies appetitive salt response in *Drosophila*. *Curr. Biol.* 32, 1776–1787.e4. <https://doi.org/10.1016/j.cub.2022.02.063>.
- McDowell, S.A.T., Stanley, M., and Gordon, M.D. (2022). A molecular mechanism for high salt taste in *Drosophila*. *Curr. Biol.* 32, 3070–3081.e5. <https://doi.org/10.1016/j.cub.2022.06.012>.
- Liu, L., Leonard, A.S., Motto, D.G., Feller, M.A., Price, M.P., Johnson, W.A., and Welsh, M.J. (2003). Contribution of *Drosophila* DEG/ENaC genes to salt taste. *Neuron* 39, 133–146. [https://doi.org/10.1016/s0896-6273\(03\)00394-5](https://doi.org/10.1016/s0896-6273(03)00394-5).
- Alves, G., Sallé, J., Chaudy, S., Dupas, S., and Manière, G. (2014). High-NaCl perception in *Drosophila melanogaster*. *J. Neurosci.* 34, 10884–10891. <https://doi.org/10.1523/JNEUROSCI.4795-13.2014>.
- Zhang, Y.V., Ni, J., and Montell, C. (2013). The Molecular Basis for Attractive Salt-Taste Coding in *Drosophila*. *Science* 340, 1334–1338. <https://doi.org/10.1126/science.1234133>.
- Lee, M.J., Sung, H.Y., Jo, H., Kim, H.W., Choi, M.S., Kwon, J.Y., and Kang, K. (2017). Ionotropic Receptor 76b Is Required for Gustatory Aversion to Excessive Na<sup>+</sup> in *Drosophila*. *Mol. Cells* 40, 787–795. <https://doi.org/10.14348/molcells.2017.0160>.
- Sánchez-Alcañiz, J.A., Silbering, A.F., Crosset, V., Zappia, G., Sivasubramaniam, A.K., Abuin, L., Sahai, S.Y., Münch, D., Steck, K., Auer, T.O., et al. (2018). An expression atlas of variant ionotropic glutamate receptors identifies a molecular basis of carbonation sensing. *Nat. Commun.* 9, 4252. <https://doi.org/10.1038/s41467-018-06453-1>.
- Weiss, L.A., Dahanukar, A., Kwon, J.Y., Banerjee, D., and Carlson, J.R. (2011). The molecular and cellular basis of bitter taste in *Drosophila*. *Neuron* 69, 258–272. <https://doi.org/10.1016/j.neuron.2011.01.001>.
- Hiroi, M., Meunier, N., Marion-Poll, F., and Tanimura, T. (2004). Two antagonistic gustatory receptor neurons responding to sweet-salty and bitter taste in *Drosophila*. *J. Neurobiol.* 61, 333–342. <https://doi.org/10.1002/neu.20063>.
- Ahn, J.E., Chen, Y., and Amrein, H. (2017). Molecular basis of fatty acid taste in *Drosophila*. *Elife* 6, e30115. <https://doi.org/10.7554/eLife.30115>.
- Chen, Y., and Amrein, H. (2017). Ionotropic Receptors Mediate *Drosophila* Oviposition Preference through Sour Gustatory Receptor Neurons. *Curr. Biol.* 27, 2741–2750.e4. <https://doi.org/10.1016/j.cub.2017.08.003>.
- Hussain, A., Üçpınar, H.K., Zhang, M., Loschek, L.F., and Grunwald Kadow, I.C. (2016). Neuropeptides Modulate Female Chemosensory Processing upon Mating in *Drosophila*. *PLoS Biol.* 14, e1002455. <https://doi.org/10.1371/journal.pbio.1002455>.
- Shim, J., Lee, Y., Jeong, Y.T., Kim, Y., Lee, M.G., Montell, C., and Moon, S.J. (2015). The full repertoire of *Drosophila* gustatory receptors for detecting an aversive compound. *Nat. Commun.* 6, 8867. <https://doi.org/10.1038/ncomms9867>.
- Sung, H.Y., Jeong, Y.T., Lim, J.Y., Kim, H., Oh, S.M., Hwang, S.W., Kwon, J.Y., and Moon, S.J. (2017). Heterogeneity in the *Drosophila* gustatory receptor complexes that detect aversive compounds. *Nat. Commun.* 8, 1484. <https://doi.org/10.1038/s41467-017-01639-5>.
- Dey, M., Ganguly, A., and Dahanukar, A. (2023). An inhibitory mechanism for suppressing high salt intake in *Drosophila*. *Chem. Senses* 48, bjad014. <https://doi.org/10.1093/chemse/bjad014>.
- Sang, J., Dhakal, S., Shrestha, B., Nath, D.K., Kim, Y., Ganguly, A., Montell, C., and Lee, Y. (2024). A single pair of pharyngeal neurons functions as a commander to reject high salt in *Drosophila melanogaster*. *Elife* 12, RP93464. <https://doi.org/10.7554/eLife.93464>.
- Schneider, C.A., Rasband, W.S., and Eliceiri, K.W. (2012). NIH Image to ImageJ: 25 years of image analysis. *Nat. Methods* 9, 671–675. <https://doi.org/10.1038/nmeth.2089>.
- Hodgson, E.S., Lettvin, J.Y., and Roeder, K.D. (1955). Physiology of a primary chemoreceptor unit. *Science* 122, 417–418. <https://doi.org/10.1126/science.122.3166.417-a>.
- Tanimura, T., Isono, K., Takamura, T., and Shimada, I. (1982). Genetic dimorphism in the taste sensitivity to trehalose in *Drosophila melanogaster*. *J. Comp. Physiol.* 147, 433–437. <https://doi.org/10.1007/BF00612007>.
- Du, E.J., Ahn, T.J., Sung, H., Jo, H., Kim, H.W., Kim, S.T., and Kang, K. (2019). Analysis of phototoxicity taste closely correlates nucleophilicity to type 1 phototoxicity. *SA* 116, 12013–12018. <https://doi.org/10.1073/pnas.1905998116>.

STAR★METHODS

KEY RESOURCES TABLE

REAGENT or RESOURCE	SOURCE	IDENTIFIER
<b>Chemicals</b>		
NaCl	Sigma-aldrich	71376
Sucrose	Duchefa Biochemie	50809.5000
Thiocholine citrate	Sigma-aldrich	T0252
Caffeine	Sigma-aldrich	C0750
Lobeline hydrochloride	TCI	L0096
20X Phosphate-buffered saline (PBS)	Biosesang	PR2007-100-00
8% paraformaldehyde in 2X PBS	Biosesang	PC2184-050-00
Normal goat serum	Jackson immunoresearch	005-000-121
Mouse anti-GFP	Invitrogen	A11120
Chicken anti-GFP	Invitrogen	A11122
Rabbit anti-RFP	Chemicon international	AB3216
Goat anti-mouse Alexa 488	Invitrogen	A11001
Goat anti-chicken Alexa 405	Invitrogen	A48260
Goat anti-rabbit Alexa 568	Invitrogen	A11011
<b>Experimental models: Organisms/strains</b>		
wCS	Lee et al. 2017	N/A
UAS-Kir 2.1	Bloomington Drosophila Stock Center	RRID: BDSC6595
Gr64f-GAL4	John Carlson lab, Yale University	N/A
ppk23-GAL4	Bloomington Drosophila Stock Center	RRID: BDSC93026
ppk28-GAL4	Bloomington Drosophila Stock Center	RRID: BDSC93020
Ir94e-GAL4	Bloomington Drosophila Stock Center	RRID: BDSC81246
Ir76b-GAL4	Bloomington Drosophila Stock Center	RRID: BDSC51311
Gr89a-GAL4	John Carlson lab, Yale University	N/A
Ir56b-GAL4	Bloomington Drosophila Stock Center	RRID: BDSC60706
Gr64f-lexA	Bloomington Drosophila Stock Center	RRID: BDSC93445
Ir76b <sup>1</sup>	Bloomington Drosophila Stock Center	RRID: BDSC51309
UAS-Ir76b	Bloomington Drosophila Stock Center	RRID: BDSC52610
UAS-Ir25a	Bloomington Drosophila Stock Center	RRID: BDSC41747
Ir56b <sup>MB09950</sup>	Bloomington Drosophila Stock Center	RRID: BDSC27818
<b>Drosophila: UAS-RNAi line</b>		
Ir7a	Vienna Drosophila Resource Center	RRID: v108171
Ir7b	Vienna Drosophila Resource Center	RRID: v100498
Ir7c	Vienna Drosophila Resource Center	RRID: v109485
Ir7f	Vienna Drosophila Resource Center	RRID: v8169
Ir7g	Vienna Drosophila Resource Center	RRID: v100885
Ir8a	Bloomington Drosophila Stock Center	RRID: BDSC25813
Ir10a	Bloomington Drosophila Stock Center	RRID: BDSC61842
Ir11a	Bloomington Drosophila Stock Center	RRID: BDSC61898
Ir20a	Vienna Drosophila Resource Center	RRID: v8658
Ir21a	Bloomington Drosophila Stock Center	RRID: BDSC64578

(Continued on next page)

**Continued**

REAGENT or RESOURCE	SOURCE	IDENTIFIER
lr25a	Bloomington Drosophila Stock Center	RRID: BDSC29539
lr31a	Vienna Drosophila Resource Center	RRID: v100345
lr40a	Bloomington Drosophila Stock Center	RRID: BDSC57566
lr41a	Bloomington Drosophila Stock Center	RRID: BDSC 58056
lr47a	Vienna Drosophila Resource Center	RRID: v11812
lr48b	Vienna Drosophila Resource Center	RRID: v107565
lr48c	Vienna Drosophila Resource Center	RRID: v45696
lr51b	Vienna Drosophila Resource Center	RRID: v29984
lr52a	Vienna Drosophila Resource Center	RRID: v37173
lr52b	Vienna Drosophila Resource Center	RRID: v26817
lr52c	Vienna Drosophila Resource Center	RRID: v330601
lr52d	Vienna Drosophila Resource Center	RRID: v8963
lr54a	Vienna Drosophila Resource Center	RRID: v47091
lr56a	Vienna Drosophila Resource Center	RRID: v109691
lr56b	Vienna Drosophila Resource Center	RRID: v4704
lr56c	Vienna Drosophila Resource Center	RRID: v107633
lr56d	Vienna Drosophila Resource Center	RRID: v6112
lr60a	Vienna Drosophila Resource Center	RRID: v3616
lr60b	Vienna Drosophila Resource Center	RRID: v12089
lr60e	Vienna Drosophila Resource Center	RRID:101261
lr62a	Bloomington Drosophila Stock Center	RRID: BDSC51026
lr64a	Vienna Drosophila Resource Center	RRID: v9011
lr67a	Vienna Drosophila Resource Center	RRID: v100644
lr67b	Vienna Drosophila Resource Center	RRID: v109462
lr67c	Vienna Drosophila Resource Center	RRID: v107921
lr68a	Bloomington Drosophila Stock Center	RRID: BDSC60108
lr68b	Bloomington Drosophila Stock Center	RRID: BDSC65360
lr75a	Vienna Drosophila Resource Center	RRID: v104136
lr75b	Bloomington Drosophila Stock Center	RRID: BDSC77143
lr75c	Vienna Drosophila Resource Center	RRID: v101682
lr75d	Vienna Drosophila Resource Center	RRID: v106286
lr76a	Bloomington Drosophila Stock Center	RRID: BDSC34678
lr76b	Bloomington Drosophila Stock Center	RRID: BDSC54846
lr84a	Bloomington Drosophila Stock Center	RRID: BDSC63992
lr85a	Bloomington Drosophila Stock Center	RRID: BDSC57772
lr87a	Bloomington Drosophila Stock Center	RRID: BDSC60476
lr92a	Bloomington Drosophila Stock Center	RRID: BDSC58205
lr93a	Bloomington Drosophila Stock Center	RRID: BDSC63700
lr94a	Vienna Drosophila Resource Center	RRID: v107734
lr94c	Vienna Drosophila Resource Center	RRID: v6817
lr94d	Vienna Drosophila Resource Center	RRID: v330479
lr94e	Vienna Drosophila Resource Center	RRID: v330650
lr94f	Vienna Drosophila Resource Center	RRID: v109702
lr94g	Vienna Drosophila Resource Center	RRID: v107901
lr94h	Vienna Drosophila Resource Center	RRID: v100407

(Continued on next page)

**Continued**

REAGENT or RESOURCE	SOURCE	IDENTIFIER
<i>Ir100a</i>	Vienna Drosophila Resource Center	RRID: v102826
<i>Nach</i>	Bloomington Drosophila Center Stock	RRID: BDSC27262
<i>Ppk</i>	Bloomington Drosophila Stock Center	RRID: BDSC29571
<i>ppk3</i>	Bloomington Drosophila Stock Center	RRID: BDSC61945
<i>ppk5</i>	Bloomington Drosophila Stock Center	RRID: BDSC25816
<i>ppk6</i>	Bloomington Drosophila Stock Center	RRID: BDSC25880
<i>ppk7</i>	Bloomington Drosophila Stock Center	RRID: BDSC25922
<i>ppk8</i>	Bloomington Drosophila Stock Center	RRID: BDSC25814
<i>ppk9</i>	Bloomington Drosophila Stock Center	RRID: BDSC25892
<i>ppk10</i>	Bloomington Drosophila Stock Center	RRID: BDSC27256
<i>ppk11</i>	Bloomington Drosophila Stock Center	RRID: BDSC26253
<i>ppk12</i>	Bloomington Drosophila Stock Center	RRID: BDSC27092
<i>ppk13</i>	Bloomington Drosophila Stock Center	RRID: BDSC25817
<i>ppk15</i>	Bloomington Drosophila Stock Center	RRID: BDSC28012
<i>ppk16</i>	Bloomington Drosophila Stock Center	RRID: BDSC25890
<i>ppk17</i>	Vienna Drosophila Resource Center	RRID: v109927
<i>ppk18</i>	Bloomington Drosophila Stock Center	RRID: BDSC25883
<i>ppk19</i>	Bloomington Drosophila Stock Center	RRID: BDSC25887
<i>ppk20</i>	Bloomington Drosophila Stock Center	RRID: BDSC25897
<i>ppk21</i>	Bloomington Drosophila Stock Center	RRID: BDSC25849
<i>ppk22</i>	Bloomington Drosophila Stock Center	RRID: BDSC28706
<i>ppk23</i>	Bloomington Drosophila Stock Center	RRID: BDSC28350
<i>ppk24</i>	Bloomington Drosophila Stock Center	RRID: BDSC26006
<i>ppk25</i>	Bloomington Drosophila Stock Center	RRID: BDSC27088
<i>ppk26</i>	Bloomington Drosophila Stock Center	RRID: BDSC25825
<i>ppk27</i>	Bloomington Drosophila Stock Center	RRID: BDSC27239
<i>ppk28</i>	Bloomington Drosophila Stock Center	RRID: BDSC 31878
<i>ppk29</i>	Bloomington Drosophila Stock Center	RRID: BDSC27241
<i>ppk30</i>	Bloomington Drosophila Stock Center	RRID: BDSC25810
<i>ppk31</i>	Bloomington Drosophila Stock Center	RRID: BDSC27087
<i>Rpk</i>	Bloomington Drosophila Stock Center	RRID: BDSC25847

**Software and algorithm**

Prism 9	GraphPad	<a href="https://www.graphpad.com/">https://www.graphpad.com/</a>
LabChart 8	ADInstruments	<a href="https://www.adinstruments.com/">https://www.adinstruments.com/</a>
ImageJ	Schneider et al. <sup>29</sup>	<a href="https://imagej.net/ij/">https://imagej.net/ij/</a>
Adobe Illustrator	Adobe	<a href="https://www.adobe.com/">https://www.adobe.com/</a>

**RESOURCE AVAILABILITY****Lead contact**

Further information and requests for resources and reagents should be directed to and will be fulfilled by the lead contact, Jae Young Kwon ([jykwon@skku.edu](mailto:jykwon@skku.edu)).

**Materials availability**

All *Drosophila* strains are available from the [lead contact](#).

**Data and code availability**

All data reported in this paper will be shared by the [lead contact](#) upon request.

This paper does not report original code.

Any additional information will be made available upon request from the [lead contact](#).

### Drosophila stocks and transgenic flies

Flies were cultured on standard cornmeal agar medium at room temperature ( $23 \pm 2^\circ\text{C}$ ). The wCS line used as a control for all experiments, is  $w^{1118}$  backcrossed to *D. melanogaster* Canton S. To construct the UAS-*Ir56b* flies used to rescue the *Ir56b* mutant, the *Ir56b* genomic region was amplified using wCS genomic DNA as a template, and cloned into the *SST13* UAS vector. Details of *Drosophila* strains used are in the [key resources table](#). CRISPR/Cas9 was used to generate the *Ir* mutants (*Ir7c*, *Ir11a*, *Ir47a*, *Ir56a*, *Ir56b*, *Ir87a*, *Ir94b*, *Ir94d* and *Ir94e*). For example, to generate the *Ir7c* mutant, two targeting plasmids were constructed, using the following oligonucleotides, 5'-CTTCGCCGCCCTGGGCAGATCATC-3' and 5'-AAACGATGATCTGCCAGGGCGGC-3', and 5'-CTTCGCGAATCGATCGTCTAATCA-3' and 5'-AAACTGATTAGACGATCATTTCGC-3', and ligating the annealed products into pU6-BbsI-chiRNA. 250 ng/ $\mu\text{l}$  of each plasmid was mixed together and injected into CAS-0001 ( $y^2\text{cho}^2v^1$ ; attP40[nos-Cas9]/CyO) embryos. The emerging adult flies were crossed with a balancer stock and PCR was used to isolate mutants with deletions between the two target sequences, and the break points were verified by sequencing. We isolated several deletion alleles which have a 1,554 bp deletion covering the 1st exon of *Ir7c*. In a similar manner, we generated other *Ir* mutants, and the table below lists the primer sets used and deletion sizes for each *Ir* mutant.

MUTANTS			Size of deletion (bp)
<i>Ir7c</i> <sup>1</sup>	frw' primer 5'-3'	CTTCGCCGCCCTGGGCAGATCATC	1,554
	rev' primer 5'-3'	AAACGATGATCTGCCAGGGCGGC	
	frw' primer 5'-3'	CTTCGCGAATCGATCGTCTAATCA	
	rev' primer 5'-3'	AAACTGATTAGACGATCATTTCGC	
<i>Ir11a</i> <sup>1</sup>	frw' primer 5'-3'	CTTCTCAGGTTGGGATATGGGTTCG	302
	rev' primer 5'-3'	AAACCGACCCATATCCCAACCTGA	
	frw' primer 5'-3'	CTTCCTGGGAGTACACACTCTTCG	
	rev' primer 5'-3'	AAACCGAAGAGTGTGTACTCCAG	
<i>Ir47a</i> <sup>1</sup>	frw' primer 5'-3'	CTTCGGCAAATAAAACTCTTAGTC	2,820
	rev' primer 5'-3'	AAACGACTAAGAGTTTTATTTGCC	
	frw' primer 5'-3'	CTTCGGATATATTTCTCTCATCAT	
	rev' primer 5'-3'	AAACATGATGAGAGAAATATATCC	
<i>Ir56a</i> <sup>1</sup>	frw' primer 5'-3'	CTTCGGCAATATGCAGATTCCATT	707
	rev' primer 5'-3'	AAACAATGGAATCTGCATATTGCC	
	frw' primer 5'-3'	CTTCGCAAGCGGATGTGACTGGCG	
	rev' primer 5'-3'	AAACCGCCAGTCACATCCGCTTGC	
<i>Ir56b</i> <sup>1</sup>	frw' primer 5'-3'	CTTCGTGCTTACTATCTCCATGT	1,025
	rev' primer 5'-3'	AAACACATGGAGATAGTCAAGCAC	
	frw' primer 5'-3'	CTTCGGATAAGACAATCCACGCCG	
	rev' primer 5'-3'	AAACCGGCGTGGATTGTCTTATCC	
<i>Ir87a</i> <sup>1</sup>	frw' primer 5'-3'	CTTCGAGCAACGTTTTTGGTTGGCGG	700
	rev' primer 5'-3'	AAACCCGCCAACCAAAAACGTTGCTC	
	frw' primer 5'-3'	CTTCTGTTCTCCATCTCCCTCCTCC	
	rev' primer 5'-3'	AAACGGAGGAGGGAGATGGAGAAC	
<i>Ir94b</i> <sup>1</sup>	frw' primer 5'-3'	CTTCGATTAATCATAAAGTGTCT	1,824
	rev' primer 5'-3'	AAACAGAACACTTTATGATTAATC	
	frw' primer 5'-3'	CTTCGTCAAGTGTCAATAGAAAAG	
	rev' primer 5'-3'	AAACCTTTCTATTGAACACTTGAC	
<i>Ir94d</i> <sup>1</sup>	frw' primer 5'-3'	CTTCGCCTTGGTTCTCCTTAGTCC	2,160
	rev' primer 5'-3'	AAACGGACTAAGGAGAACCAAGGC	
	frw' primer 5'-3'	CTTCGCGCTTTGGGGATGGATGC	
	rev' primer 5'-3'	AAACGCATCCATCCACAAAGCGC	

(Continued on next page)



**Continued**

MUTANTS			Size of deletion (bp)
IR94e <sup>1</sup>	frw' primer 5'-3'	CTTCGAATAGGAACTTTAGTCTGT	1,594
	rev' primer 5'-3'	AAACACAGACTAAAGTTCCTATTC	
	frw' primer 5'-3'	CTTCGAGTCCTCATCGTGAATTCA	
	rev' primer 5'-3'	AAACTGAATTCACGATGAGGACTC	

**Electrophysiology**

Extracellular single-unit recordings were performed using the tip-recording method.<sup>30</sup> To immobilize 3-6-day-old flies, ice was used, and they were fixed using a reference electrode containing *Drosophila* Ringer solution. Individual sensilla were exposed to tastants via a glass recording electrode (1020 μm diameter) filled with tastant solution dissolved in 30 mM tricholine citrate. LabChart 8 software (ADInstrument) was used to analyze neuronal firing rates, by counting the number of spikes obtained in the first 500 ms after contact. When conducting the RNAi screen, we measured physiological responses to NaCl in L3 and L4 for the L-type sensilla, and in S4 and S8 for the S-c type sensilla. We observed that sensilla of the same type showed very similar responses. Therefore, in Figure 2 and Figure S3, we presented only the results for L3 and S4. To avoid prolonged stimulation with NaCl, electrophysiological recordings of individual labellar taste sensilla were limited to within 10 sec of stimulating with NaCl.

**Behavioral assays**

The binary choice assay was performed with minor modifications of the original protocol.<sup>31</sup> Briefly, 1 to 3-day-old flies were collected in groups of 50 males and placed in a fresh vial for 1 day. Flies were starved for 24 h in a 1% agarose vial prior to the assay. Tastants were mixed into 1% agarose containing either blue dye (Brilliant Blue FCF, wako, 0.125 mg ml<sup>-1</sup>) or red dye (sulforhodamine B, sigma, 0.5 mg ml<sup>-1</sup>). 72-well plate dishes were filled with tastant in alternating color patterns. Starved flies were transferred to the 72-well plate dishes and allowed to feed for 90 min at room temperature in the dark. The fed flies were frozen at -20 °C and the number of flies which fed on a particular tastant was counted under a dissection microscope by observing the abdomens of the flies. A preference index (PI) was calculated by the equation:  $(N_R + N_P/2)/(N_R + N_P + N_B)$  or  $(N_B + N_P/2)/(N_R + N_P + N_B)$ , where  $N_R$  is the number of red,  $N_P$  is the number of purple, and  $N_B$  is the number of blue abdomens. PI 1 means complete preference and 0 means complete avoidance to the food. PI 0.5 means no preference for both foods. No effects were observed for the dyes alone.

**S2 cell culture and transfection**

*Drosophila* S2 cells were cultured in Schneider's *Drosophila* medium (Gibco) with 10% FBS (Invitrogen) and 0.2% penicillin/streptomycin (HyClone) at room temperature, zero CO<sub>2</sub> condition. The cells were subcultured twice a week at a density of half or one third. S2 cells in a 35 mm cell culture dish at 60-80% cell confluency were transfected by the calcium phosphate method. IR56b TTC, IR76b cDNA, and IR25a cDNA were synthesized by Integrated DNA Technologies, and inserted into the SST13 UAS vector. We transfected cells with pActin5c-GAL4, pUAST-EGFP and the three IR plasmids. Plasmid (μg): pActin5c-GAL4 (1.5), pUAST-EGFP (1.5), pSST13-IR25a (2.7), pSST13-IR56b (1.35), and pSST13-IR76b (1.35). Briefly, carefully mix 2X HBS solution and 2M calcium phosphate solution, add distilled water and plasmid. Incubate the mixed transfection solution at room temperature for 30 min. Add incubated transfection solution dropwise to culture dish. After 4~6 hours, remove medium containing calcium phosphate and wash cells twice with fresh medium. Lastly, replace new medium and incubate in S2 cell culture conditions.

**Whole-cell recording of S2 cells**

The transfected S2 cells were transferred onto coverslip chips coated with 0.1 mg/mL poly-L-lysine (Sigma). After 6-12 hours, only GFP-positive cells were selected for patch clamp experiments using fluorescent microscopy. Whole-cell recording is performed at room temperature (22-25°C). Electrodes were pulled from borosilicate glass micropipette capillaries (Sutter Instrument) using a P-97 micropipette puller (Sutter Instrument) with resistances of 2-4 MΩ. Whole-cell recordings were performed using a HEKA EPC-10 amplifier and Pulse software (HEKA Elektronik). The whole-cell access resistance was 2-6 MΩ, and series-resistance errors were compensated by 60%. The holding potential is 0 mV. Current is recorded by 200 ms test pulses from -100 mV to +100 mV with 20 mV increments. The extracellular solutions contained 150 mM NaCl, 10 mM HEPES, 10 mM glucose (adjusted to pH 7.4 with NaOH). The pipette solution contained 165 mM CsMes, 5 mM MgCl<sub>2</sub>, 10 mM HEPES (adjusted to pH 7.4 with CsOH).

**Whole-cell recording of HEK293T cells**

DNA of three IRs was inserted into the pcDNA3.1(+) vector for mammalian cell expression. HEK293T cells were cultured in DMEM (HyClone) with 10% FBS (Invitrogen) and 0.2% penicillin/streptomycin (HyClone) at 37°C, 5% CO<sub>2</sub>. The cells were transfected by Lipofectamine 2000 (Thermo Fisher Scientific). Other conditions of whole-cell recording were identical to those of S2 cells.

### Patch clamp in *Xenopus* oocytes

Two electrode voltage clamping (TEVC) was conducted as described elsewhere.<sup>32</sup> Briefly, oocyte-positive *Xenopus laevis* were obtained from the Korean *Xenopus* Resource Center for Research (<http://knrrb.knrc.or.kr/index.jsp?rrb=kxrcr>, Chuncheon, Republic of Korea). IR56b TTC, IR56b cDNA, IR76b cDNA, and IR25a cDNA were synthesized by Integrated DNA Technologies, and inserted into the pOX vector. cDNA was *in vitro* transcribed using the mMessage mMachinE T3 (Invitrogen, AM1348) kit according to the manufacturer's manual, for injection into oocytes. *Xenopus* oocytes defolliculated by collagenase (type 1, LS004196, Worthington, NJ, USA) and manual stripping after surgical acquisition of ovaries were microinjected with capped RNAs of interest (Nanoject II, Drummond Scientific, PA, USA). The injected oocytes were allowed to express the IR genes for three days prior to electrophysiological characterization. The initial perfusion buffer for TEVC contained 20 mM NaCl and 160 mM sorbitol together with 1 mM KCl, 1 mM MgCl<sub>2</sub>, 5 mM HEPES pH 7.6. To maintain a constant osmolarity throughout the changing NaCl concentrations, sorbitol concentrations were adjusted to 120 mM for 40 mM NaCl, 40 mM for 80 mM NaCl, and 0 mM for 100 mM NaCl. Voltage sweeps were undertaken for 300 ms every second from -60 to +60 mV, while the voltage was -60 mV before sweeps under the control of Axoclamp 900A (Molecular Devices, CA, USA). The resulting current was registered through a digitizer (Digidata 1440A, Molecular Devices). We binned recordings yielding currents at 100 mM NaCl higher than the standard deviation of the entire set of *Ir56bTTC* recordings for functional analysis such as dose dependence. If there was no binned recording, all the complete recordings were analyzed together. Other than coinjection of *Ir56bTTC* with coreceptor cRNAs, there was no current response larger than the standard deviation of the *Ir56bTTC* experiment.

### Immunostaining and microscopy

The labellums and brains of 5- to 7-day-old female flies were dissected and fixed in paraformaldehyde solution (4 % paraformaldehyde, 1 X PBS and 0.2 % Triton-X) for 1 hour at 4 °C. Samples were washed three times for 10 mins each with PBS-T solution (1 X PBS and 0.2 % Triton-X), and incubated in blocking solution (3 % goat serum in PBS-T) overnight at 4 °C. Primary antibodies were added and incubated for 2 days at 4 °C. After three washes, secondary antibodies were added for 1 day, then washed three times and mounted in mounting solution. For labellum immunostaining, mouse anti-GFP (1:500, Invitrogen) and rabbit anti-RFP (1:500, Chemicon International) were used as the primary antibodies, and goat anti-mouse Alexa 488 (1:250, Invitrogen) and goat anti-rabbit Alexa 568 (1:250, Invitrogen) were used as the secondary antibodies. For brain immunostaining, chicken anti-GFP (1:500, Invitrogen) and rabbit anti-RFP (1:500, Chemicon International) were used as the primary antibodies, and goat anti-GFP Alexa 405 (1:250, Invitrogen) and goat anti-RFP Alexa 568 (1:250, Invitrogen) were used as the secondary antibodies. All images were obtained using a spinning disk confocal microscope (Dragonfly 302, Oxford (Andor)) with a 40x oil immersion objective at a resolution of 2048 X 2048. Obtained images were processed with ImageJ.